

Experimental and NMR Theoretical Methodology Applied to Geometric Analysis of the Bioactive Clerodane *trans*-Dehydrocrotonin

Breno Almeida Soares,^a Caio Lima Firme,^{*a} Maria Aparecida Medeiros Maciel,^{a,b} Carlos R. Kaiser,^c Eduardo Schilling^d and Adailton J. Bortoluzzi^d

^aUniversidade Federal do Rio Grande do Norte, Instituto de Química,
Campus Lagoa Nova, 59072-970 Natal-RN, Brazil

^bPrograma de Pós-graduação em Biotecnologia, Universidade Potiguar Laureate International
Universities, Campus Salgado Filho, 59075-000 Natal-RN, Brazil

^cUniversidade Federal do Rio de Janeiro, Instituto de Química,
Ilha do Fundão, 21941-909 Rio de Janeiro-RJ, Brazil

^dUniversidade Federal de Santa Catarina, Departamento de Química,
Campus Universitário Trindade, 88040-900 Florianópolis-SC, Brazil

trans-Desidrocrotonina (*t*-DCTN), um bioditerpeno do tipo 19-nor-clerodano isolado de *Croton cajucara* Benth, representa um dos clerodanos da atualidade com maiores índices de investigações científicas. Neste trabalho, uma nova abordagem unindo dados de difração de raios X, dados de ressonância magnética nuclear (NMR) e dados teóricos foi aplicada para a completa caracterização da *t*-DCTN. Para tanto, a geometria de *t*-DCTN foi reavaliada por difração de raios X e NMR de ¹H e ¹³C e foi comparada com os dados teóricos obtidos por B3LYP/6-311G++(d,p). A subsequente avaliação dos valores teóricos e experimentais de deslocamentos químicos de NMR e constantes de acoplamento spin-spin apresentou correlações muito boas entre propriedades magnéticas teóricas e experimentais. Adicionalmente, os índices de deslocalização entre átomos de hidrogênio, δ(H,H'), correlacionaram bem com os dados experimentais e calculados de constante de acoplamento. Uma análise topológica complementar utilizando a teoria quântica de átomos em moléculas (QTAIM) mostrou interações intramoleculares para *t*-DCTN.

trans-Dehydrocrotonin (*t*-DCTN) a bioactive 19-nor-diterpenoid clerodane type isolated from *Croton cajucara* Benth, is one of the most investigated clerodane in the current literature. In this work, a new approach joining X-ray diffraction data, nuclear magnetic resonance (NMR) data and theoretical calculations was applied to the thorough characterization of *t*-DCTN. For that, the geometry of *t*-DCTN was reevaluated by X-ray diffraction as well as ¹H and ¹³C NMR data, whose geometrical parameters were compared to those obtained from B3LYP/6-311G++(d,p) level of theory. From the evaluation of both calculated and experimental values of ¹H and ¹³C NMR chemical shifts and spin-spin coupling constants, it was found very good correlations between theoretical and experimental magnetic properties of *t*-DCTN. Additionally, the delocalization indexes between hydrogen atoms correlated accurately with theoretical and experimental spin-spin coupling constants. An additional topological analysis from quantum theory of atoms in molecules (QTAIM) showed intramolecular interactions for *t*-DCTN.

Keywords: *Croton cajucara*, *trans*-dehydrocrotonin, NMR, DFT calculations, QTAIM, X-ray crystallography

*e-mail: firme.caio@gmail.com, caiofirme@quimica.ufrn.br

Introduction

The clerodane group of diterpenes includes more than 800 isolated compounds and a significant number showed to have biological activity such as antimicrobial,¹ psychotropic,² antiulcer³ and antitumor.⁴ Actually, the 19-nor-clerodane *trans*-dehydronerotin (*t*-DCTN), a furan clerodane skeleton type diterpene (Figure 1), is one of the most important bioactive clerodane reported in the current literature. This natural compound isolated from *Croton cajucara* Benth (Euphorbiaceae), a widely grown tree in the Amazonian region of Northern Brazil, became an important target for pre-clinical researches. In fact, pharmacological studies examining *t*-DCTN confirmed its anti-inflammatory, analgesic, antitumor, antiulcer, hypolipidemic and cardioprotective effect.^{5,6} *t*-DCTN has also been shown to have antimutagenic activity⁵⁻⁷ and did not induce clastogenic, anticlastogenic, apoptotic and cytotoxic activities.⁸

In general, a complete characterization of natural terpenoids compounds requires a large amount of work, in which 1D and 2D-nuclear magnetic resonance (NMR) techniques can be combined with X-ray diffraction analysis. Since 1976, when Ferguson and Marsh reported the first crystallographic analysis of a diterpenoid type clerodane molecule,⁹ a plenty of reports arises describing clerodane molecules by crystallographic analysis in combination with NMR techniques. Owing to the complexity of clerodane structural molecule, the X-ray diffraction analysis is an important tool for a reliable and complete structural analysis of a new natural or semi-synthetic organic compound. In this context, the use of theoretical quantum chemistry

methods becomes a complementary tool for structural analysis of organic compounds.^{3,10-26}

The NMR spectral data of a new compound provide an useful information for its molecular identity and geometry. In fact, NMR parameters such as chemical shifts and spin-spin coupling constants (SSCC), as well as theoretical calculations and ¹H spectrum simulations give support for the total characterization of complex molecules. Regarding the SSCC parameter, it plays an important role on the conformational analysis and elucidation of several types of molecules,²⁷⁻³¹ mainly when it is correlated with theoretical SSCC.³²⁻⁴³

Most of the theoretical descriptions of spin spin coupling constants follows the Ramsey and Purcell interpretation⁴⁴ and Ramsey formulation.⁴⁵ In this method, the coupling constants are calculated by adding four different terms: (1) diamagnetic spin orbit (DSO) as well as (2) the paramagnetic spin orbit (PSO), which represent the interactions of the magnetic field of the nuclei mediated by the electron orbital motion, (3) the Fermi contact (FC), which is also a response property reflecting the interaction between the electron spin magnetic moment close to the nucleus and the magnetic field at the nucleus, and (4) the spin dipole (SD), which describes the interactions between the nuclear magnetic moments as mediated by the electronic spin angular moment. For an accurate quantum chemical description of SSCCs all the terms cited above must be considered.⁴⁶⁻⁴⁹ In addition, the delocalization index between two hydrogen atoms, $\delta(H,H')$, can also be used in the theoretical analysis of the SSCCs.⁵⁰

The quantum theory of atoms in molecules (QTAIM)⁵¹ is based on an observable, the electron density, and it has been

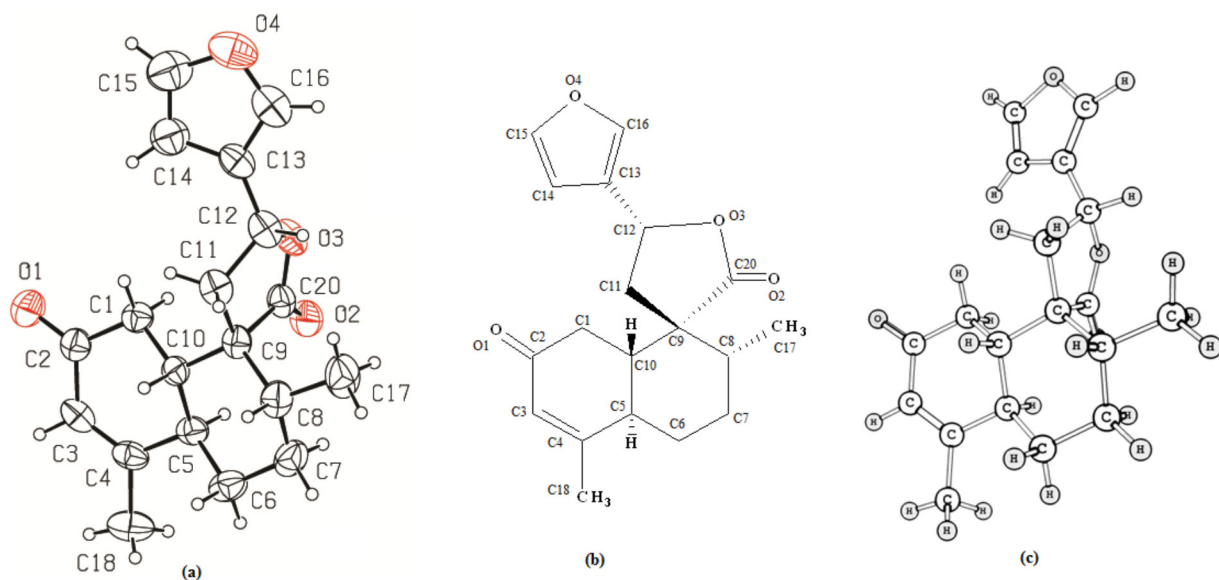


Figure 1. (a) Crystallographic structure, (b) skeleton formula and (c) optimized structure from B3LYP/6-311G++(d,p) level of theory of the clerodane *t*-DCTN.

used for several experimental applications, for example, the estimate of the intensity of infrared (IR) spectrum^{52,53} and magnetic susceptibility,⁵⁴ as well as the calculation of topological information from X-ray diffraction data⁵⁵ and the linear correlation between delocalization index $\delta(H,H')$ and proton-proton coupling constants.⁵⁶⁻⁵⁸ The linear correlation between delocalization index and fluorine fluorine coupling constants was also described.⁵⁹

Unambiguous NMR assignments for *t*-DCTN and its stereochemistry determination were previously reported using a powerful NMR equipment (600 MHz for ¹H), 2D-NMR experiments, AM1 calculations and ¹H NMR spectrum simulations.⁶⁰ In the present work, we have performed X-ray diffraction of *t*-DCTN and many theoretical calculations using B3LYP. The geometric skeleton of *t*-DCTN was re-examined by means of several correlations involving experimental and theoretical data in order to provide additional structural information such as bond length and dihedral angles measurements which are extensively used in the conformational analysis of biomolecules applied to its pharmacological responses.^{3,12,24} Correlations between theoretical results and corresponding experimental data plus topological analysis from QTAIM are herein discussed.

Experimental

Material and methods

Plant material was collected in Jacundá City located at Pará State (Amazonian region, Brazil), and identified by Nelson A. Rosa.⁵ A voucher specimen (no. 247) has been stored at the Herbarium of the Museu Paraense Emílio Goeldi (Belém, PA, Brazil). The isolation of *t*-DCTN was performed according to the literature⁵ and its recrystallization (from a mixture of hexane:ether 7:3) yielded suitable crystal for X-ray diffraction. The assignments for structure elucidation were previously determined from ¹H (600 MHz) and ¹³C (150 MHz) NMR spectroscopy.⁶⁰

Single crystal X-ray diffraction

The crystal data were measured on an Enraf-Nonius CAD4 diffractometer using graphite monochromated Mo-K α radiation ($\lambda = 0.71069 \text{ \AA}$) at room temperature. A colorless crystal with dimensions of $0.40 \times 0.33 \times 0.30 \text{ mm}$ was isolated from a homogeneous crystalline sample of *t*-DCTN. Unit-cell parameters were determined from centering of 25 reflections in the θ angle ranging from 4.92 to 12.03° and refined by the least-squares method

according to standard procedure.⁶¹ Intensities were collected using the ω -2 θ scan technique. All diffracted intensities were corrected by Lorentz and polarization effects. The structure was solved by direct methods and was refined by the full-matrix least-squares method using SIR97 and SHEXL97.^{62,63} All non-hydrogen atoms were refined with anisotropic displacement parameters. Hydrogen atoms were placed at idealized positions using standard geometric criteria. The PLATON program⁶⁴ was used to generate the picture of the molecular structure. Further relevant crystallographic data are summarized in Table 1.

Table 1. Crystal data and structure refinement for *t*-DCTN

Empirical formula	$C_{19}H_{22}O_4$
Formula weight	314.37
Temperature / K	293(2)
Wavelength / \AA	0.71073
Crystal system	Orthorhombic
Space group	$P2_12_12_1$
a / \AA	7.3869(8)
b / \AA	13.8966(13)
c / \AA	16.018(3)
Volume / \AA^3	1644.3(4)
Z	4
ρ / (g cm ⁻³)	1.270
μ / mm ⁻¹	0.088
F(000)	672
Crystal size	$0.40 \times 0.33 \times 0.30 \text{ mm}^3$
Theta range for data collection	1.94 to 27.97°
Index ranges	$-9 \leq h \leq 0$. $-18 \leq k \leq 0$. $-21 \leq l \leq 0$
Reflections collected / unique	2184 / 2184 [R(int) = 0.0000]
Completeness to theta = 27.97°	96.2 %
Absorption correction	None
Refinement method	Full-matrix least-squares on F ²
Data / restraints / parameters	2184 / 0 / 208
Goodness-of-fit on F ²	0.982
Final R indices [I > 2σ(I)]	R1 = 0.0502; wR2 = 0.1076
R indices (all data)	R1 = 0.1753; wR2 = 0.1386
Largest diff. peak and hole / (e \AA^{-3})	0.170 and -0.105

Crystallographic data (atomic coordinates and equivalent isotropic displacement parameters, calculated hydrogen atom parameters, anisotropic thermal parameters and bond lengths and angles) have been deposited at the Cambridge Crystallographic Data Center (deposition number CCDC 276648). Copies of this information may be obtained free of charge from: CCDC, 12 Union Road, Cambridge, CB2 1EZ, UK (Fax: +44-1223-336-033; e-mail: deposit@ccdc.cam.ac.uk or <http://www.ccdc.cam.ac.uk>).

Computational details

The geometry of the studied species was optimized using standard techniques.⁶⁵ Vibrational analysis of *t*-DCTN optimized geometry was carried out to determine whether it was a true minimum or a transition state. No imaginary frequency was obtained confirming that a minimum was found in the potential energy surface. The calculations were performed at B3LYP/6-311G++(d,p)⁶⁶⁻⁷¹ using GAUSSIAN 09 package.⁷² From the Kohn-Sham orbitals of *t*-DCTN optimized structure, the electron density was obtained and then used for the calculation of *t*-DCTN topological data by means of the AIM2000 software.⁷³

Results and Discussion

The DFT procedures for computing proton-proton coupling constants and/or chemical shifts of unknown structures or targets from synthetic studies, have been extensively reported.³²⁻³⁸ In this work, aiming to describe the most stable conformational status of *t*-DCTN (Figure 1) more thoroughly, we have examined the combined set of X-ray data, NMR spectra and computational calculations using B3LYP/6-311G++(d,p) level of theory. A single crystal X-ray diffraction was undertaken in order to re-examine the asymmetric centers (C5, C8, C9, C10 and C12) of *t*-DCTN. The PLATON perspective drawing (Figure 1a) is in agreement with the geometric configuration supported by NMR spectra of *t*-DCTN. The theoretical analysis of geometric and magnetic properties of *t*-DCTN gives additional support for its experimental characterization since it confirms the structure of the most stable conformer of *t*-DCTN.

Figure 1 shows the crystallographic structure of *t*-DCTN (Figure 1a), the corresponding skeleton formula (Figure 1b) and its optimized structure obtained from B3LYP/6-311G++(d,p) (Figure 1c). In the perspective drawing (Figure 1a and 1c), the conformation of the decalin system chair is distorted due to $\Delta^{3,4}$ double bond (located at C3 and C4 in the so-called ring A) and also the spiro-lactone at C9 (in the so-called ring B).

Geometrical data available in the Supplementary Information indicate that the hydrogen atoms at C10 and C5 positions are on the opposite side of A/B decalin system, assuming *trans* configuration (Table S1 from Supplementary Information). In addition, the bond lengths and angles are as expected for a *trans* geometry for *t*-DCTN.

The existence of the spiro arrangement in lactone moiety can be noticed by the fact that C9 is shared by the lactone group itself and also by ring B of decalin system. The α,β -unsaturated carbonyl group located in C2, C3, C4

and O1 atoms of decalin ring A could be observed revealing similar bond lengths of 3-(4-chloro-benzene-sulfonamido)-5-methyl-cyclo-hex-2-en-1-one, whose geometric and topological parameters were described by Jackson and co-workers.⁷⁴ The C=O, C=C and C–C bond lengths of 3-(4-chloro-benzene-sulfonamido)-5-methyl-cyclo-hex-2-en-1-one (1.251, 1.356 and 1.437 Å, respectively) are comparable to those corresponding bonds in ring A of *t*-DCTN (1.215, 1.325 and 1.449 Å, respectively).

The minimum in the potential energy surface of *t*-DCTN was obtained by B3LYP/6-311G++(d,p) level of theory whose geometrical parameters were compared with those from X-ray diffraction (Table S1 from Supplementary Information). The theoretical and experimental parameters for *t*-DCTN are very similar, except for some angle values from furan and lactone moieties. The O3–C12–C11, C15–C14–C13 and C13–C16–C14 angles have nearly two degrees of discrepancy when comparing theoretical and experimental results (See Supplementary Information). The root mean square deviation (RMSD) of *t*-DCTN bond lengths and bond angles was calculated in order to measure the accuracy of theoretical results in comparison with X-ray data. The RMSD values are 0.0153 and 0.9333 for bond lengths and bond angles, respectively. These values show the precision of the chosen level of theory for geometric calculations of *t*-DCTN and also indicate the relatively smaller precision of calculated bond angles with respect to experimental values.

As a consequence of agreement between experimental and theoretical results, Figure 1a (PLATON thermal ellipsoids plots) and Figure 1c (an optimized structure) indicate similar nuclear configuration for *t*-DCTN. Both stereo views showed a visual similarity in arrangements of the decalin and lactone moieties, as well as for furan ring, which is out of plane for both representations.

Theoretical magnetic properties (chemical shifts and SSCC) of *t*-DCTN were obtained from B3LYP/6-311G++(d,p) level of theory and compared with corresponding experimental values (See Supplementary Information).

Aiming to reinforce the discussion on the absolute configuration of *t*-DCTN, correlations between the experimental NMR data⁶⁰ and theoretical NMR chemical shifts of *t*-DCTN are presented in Figures 2a (¹H NMR chemical shifts, in ppm) and 2b (¹³C NMR chemical shifts, in ppm). Thereby we found very good linear correlations between the experimental and theoretical NMR chemical shifts as indicated by their corresponding coefficient of determinations. The agreement between experimental (both X-ray and NMR data) and the corresponding theoretical data from our applied computational protocol, indicate

that B3LYP/6-311G++(d,p) level of theory suffices for the analysis of magnetic and geometric properties of the evaluated clerodane *t*-DCTN.

The vicinal or long range coupling constants of *t*-DCTN were calculated from the gauge-independent atomic orbital (GIAO) method including the four contributing terms (FC, PSO, DSO, SD)⁴⁶ at the B3LYP/6-311G++(d,p) level of theory. The B3LYP/GIAO method provides accurate coupling constant values in many systems, being most of them related to rigid structure and/or aromatic molecular systems.³⁷⁻⁴⁰

A reasonably good correlation between calculated and experimental coupling constants was obtained (Figure 3), except for those values involving hydrogen atoms 8 and 17, whose differences between experimental and theoretical values were larger than three ppm. Therefore, the B3LYP/6-311G++(d,p)/GIAO method, including the four contributing terms (FC, PSO, DSO, SD), suffices to describe magnetic properties of low symmetry and flexible structures similar to *t*-DCTN.

The delocalization index from QTAIM is the quantity of shared electrons in an atomic pair, bonded or non-bonded,

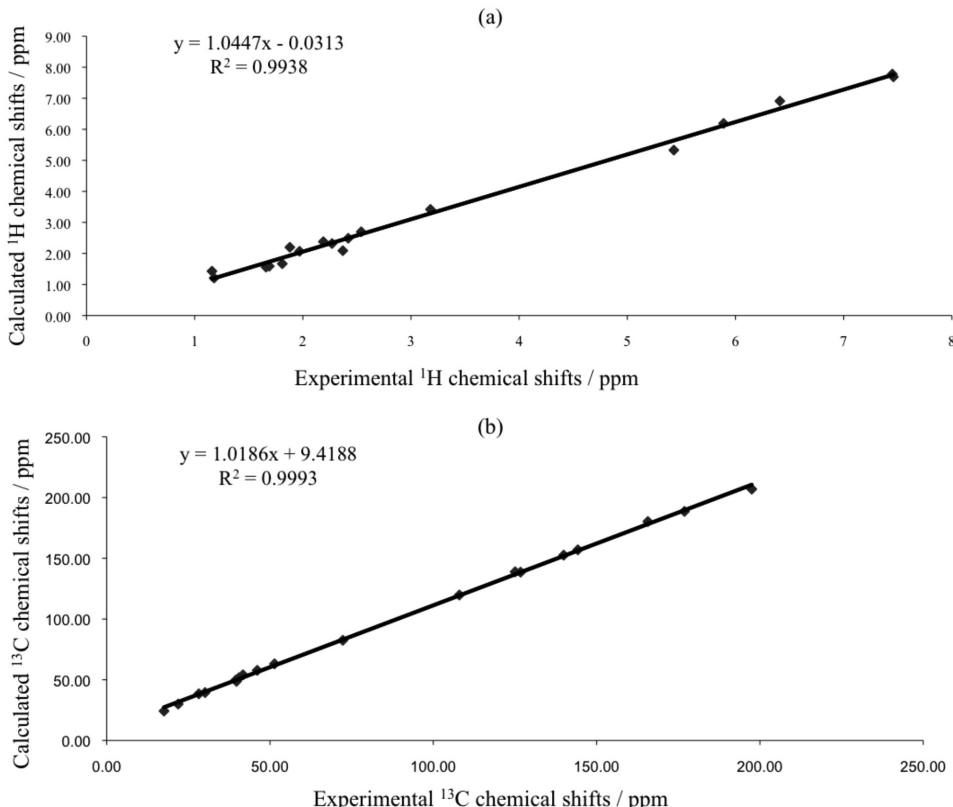


Figure 2. (a) Plot of experimental vs. calculated (B3LYP/6-311G++(d,p)) ¹H NMR chemical shifts and (b) plot of experimental vs. theoretical ¹³C NMR chemical shifts for *t*-DCTN.

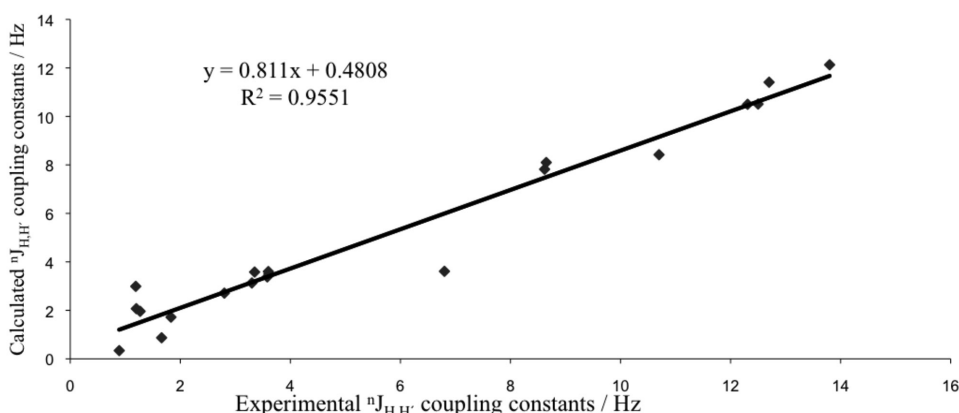


Figure 3. Plot of experimental vs. calculated (B3LYP/6-311G++(d,p)) ¹H vicinal or long range NMR spin-spin coupling constants [ⁿJ (H,H')] for *t*-DCTN.

and it has been used to establish a relation with coupling constants of many molecular systems.⁵⁶ There are excellent correlations observed in literature^{37,56-58} between delocalization index of vicinal or long range hydrogen atoms $\delta(H,H')$ and corresponding experimental coupling constants. Additionally, fluorine fluorine coupling constants also showed satisfactory correlation with delocalization index data for aromatic systems.⁵⁹

Figures 4a and 4b shows the plots of experimental and theoretical coupling constants versus corresponding delocalization index of vicinal or long range hydrogen atoms of *t*-DCTN, respectively. Both of them give a reasonably good coefficient of determination, meaning that the amount of shared charge density between long or vicinal hydrogen atoms is related with the magnitude of the corresponding coupling constant, i.e., a relation between electronic and magnetic properties of *t*-DCTN is established in Figure 4. According to Gutowsky and collaborators,⁷⁵ the spin-spin coupling arises from second-order interaction between the nuclear magnetic moments and some magnetic field internal to the molecule through electrons along chemical bonding. The results from Figure 4 suggest that the influence of weak electron interaction, through field

effect, between the interacting nuclei plays some role in long range or vicinal spin-spin coupling as well, which concords with J-couplings in hydrogen bonds.^{76,77}

Aiming at the investigation of possible intramolecular interactions in *t*-DCTN, we also carried out its topological analysis based on the gradient of the charge density distribution. Figure 5 shows the molecular graph of *t*-DCTN which contains critical points of the charge density and bond paths. Critical point is a mathematical point of a determined function, whose gradients, with respect to their coordinates, are zero. The topology of charge density may have four types of critical points: the nuclear attractor critical point (where it is located an atomic nucleus), the bond critical point (a critical point between two linking atoms), the ring critical point (a critical point within a ring) and the cage critical point (a critical point inside a molecular cage). The bond path is an atomic interaction line linking two nuclear critical points (or atomic basins) and one bond critical point between them. It corresponds to the maximum charge density compared to vicinal transversal region.⁵¹

Figure 5 shows the molecular graph of the *t*-DCTN which has five bond critical points associated with

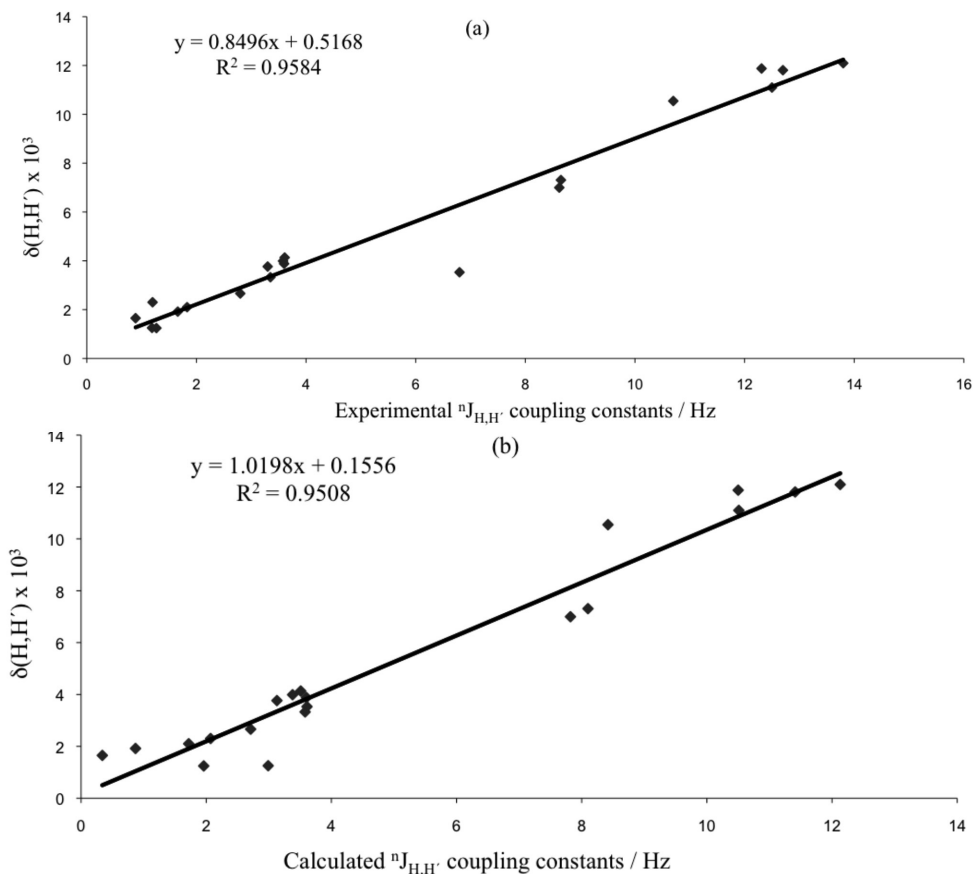


Figure 4. (a) Plot of experimental spin-spin coupling constants of vicinal or long range protons [$J^n(H,H')$] vs. corresponding delocalization index values $\delta(H,H')$; (b) plot of calculated spin-spin coupling constants (B3LYP/6-311G++(d,p)) vs. corresponding delocalization index $\delta(H,H')$ for *t*-DCTN.

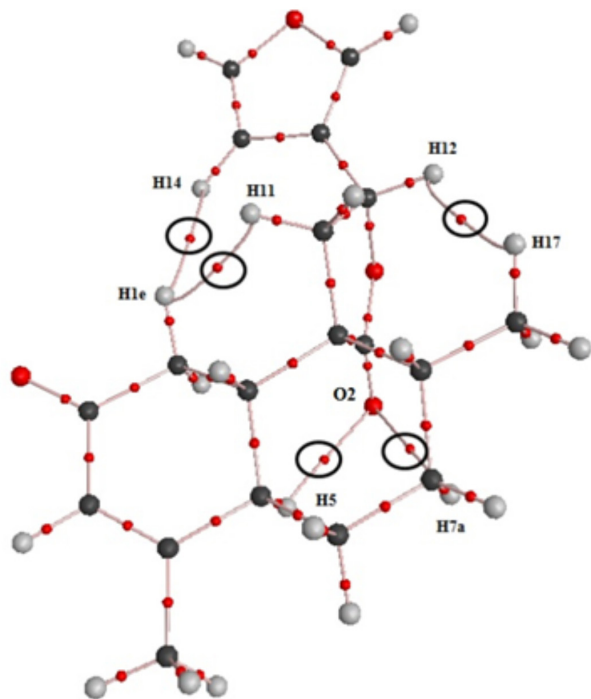


Figure 5. Molecular graph for *t*-DCTN indicating the bond paths analyzed in Table 2.

intramolecular closed-shell interactions, where three out of them are hydrogen-hydrogen bonds (Table 2).

An important applicability of QTAIM is to quantify and qualify bonded interactions based on five topological parameters obtained at the analyzed bond critical point:⁷⁸⁻⁸¹ (1) the value of the charge density of the critical point (ρ_b); (2) the value and the sign of the Laplacian ($\nabla^2\rho$) of the charge density; (3) the ratio $|\lambda_1|/\lambda_3$, where λ_1 and λ_3 are eigenvalues of Hessian matrix of the charge density; (4) the ratio G_b / ρ_b , where G_b is the kinetic energy density; and (5) the total energy density (H_b) at the bond critical point. In the case where $\nabla^2\rho > 0$, ρ_b is relatively low ($\rho_b < 6 \times 10^{-2}$ a.u.), the ratio $|\lambda_1|/\lambda_3 < 1$, the ratio $G_b / \rho_b > 1$ or close to 1, and H_b has a positive value, close to zero, the chemical interaction is defined as closed shell interaction and it corresponds, for example, to hydrogen bond, ionic bond and van der Waals interactions.⁷⁸⁻⁸¹ Table 2 shows these five topological data for all intramolecular bonded interaction in *t*-DCTN

(Figure 5) which are certainly related to the highest stability of *t*-DCTN found in its NMR and X-ray data.

All values in Table 2 are in agreement with the topological characterization of closed shell interaction for the five interatomic interactions.⁷⁸⁻⁸¹ The values of G_b / ρ_b in Table 2 are in the same range to that found in closed shell interactions in metallocenes, involving metal atom and π ligand carbon atom.⁸² The most stable conformer of *t*-DCTN presents five intramolecular interactions: three H-H bonds, linking hydrogen atoms from decalin system to hydrogen atoms from spiro-lactone and furan rings, and two (C)O--H(C) bonded interactions linking the lactone carbonyl oxygen to two axial hydrogen atoms from decalin ring. It is demonstrated in literature that H-H bonding contributes as a stabilizing factor to the energy of a chemical system.^{81,83} Matta and co-workers have investigated intramolecular H-H bonding in several compounds showing its stabilizing effect whose values of the five topological parameters listed in Table 2 were similar to the H-H bonds in *t*-DCTN.

Regarding the (C)O--H(C) bonded interactions we compared the charge density of bond critical points and Laplacian of the charge density between (C)O--H(C) bonded interactions and the corresponding values from hydrogen bonds (O-HO) of substituted malonaldehyde enols.⁸⁴ The charge density of (C)O--H(C) bonded interactions are nearly one-fifth of the averaged charge density value of hydrogen bonds of substituted malonaldehyde enols. On the other hand, according to less positive values of $\nabla^2\rho$ of the bond critical point related to (C)O--H(C) bonded interactions in *t*-DCTN, the corresponding distribution of the charge density is less dispersed in (C)O--H(C) bonded interactions in *t*-DCTN than that in hydrogen bonds of substituted malonaldehyde enols.⁸⁴

Therefore, the sum of the charge density in the five intramolecular interactions in *t*-DCTN is nearly equivalent to the charge density of one hydrogen bond of malonaldehyde enol,⁸⁴ which shows the cooperative effect of the five weak intramolecular interactions in determining the most stable conformer of *t*-DCTN. Three intramolecular interactions (H-H bonds) are not influenced by polarity

Table 2. Values of the charge density of bond critical points (ρ_b), the corresponding Laplacian of the charge density ($\nabla^2\rho$), the ratio $|\lambda_1| / \lambda_3$, the ratio G_b / ρ_b , and the total energy density (H_b) of all intramolecular bonded interactions in *t*-DCTN

Interactions	$\rho_b \times 10^2$ / a.u.	$\nabla^2\rho$ / a.u.	$ \lambda_1 / \lambda_3$	G_b / ρ_b	$H_b \times 10^2$ / a.u.
H1e-H11	1.285	0.045	0.194	0.721	1.653
H1e-H14	0.384	0.012	0.175	0.632	0.487
H17-H12	0.771	0.026	0.162	0.705	0.971
O2-H7a	0.882	0.029	0.167	0.722	1.186
O2-H5	1.139	0.036	0.184	0.707	1.512

while it influences the other two interactions involving oxygen atom. Indeed, the most stable conformer of *t*-DCTN is the one obtained by means of NMR and X-ray whose experimental values are in very good agreement with the corresponding theoretical data. Then, our theoretical calculations reinforced the characterization of the most stable conformer and also enabled a clear understanding of the electronic structure of *t*-DCTN.

Currently, there is a number of *Croton cajucara* Benth researches devoted to its chemical, biochemical, pharmacological and more recently potential advantages of molecular incorporation into drug delivery systems, specifically DCTN-load studies.⁸⁵⁻⁸⁸ In fact, concerning to the biotechnological advanced context, our recent work reported to *trans*-dehydrocrotonin cover its encapsulation in liposomes with a significant enhancement of the antitumor activity of this 19-*nor*-clerodane-type diterpene.⁸⁵ Since the stability of *t*-DCTN loaded in different biological formulations had been investigated aiming its pharmacologic improvement, this present work attracts significant importance on physicochemical characteristics of this compound to be applied in the advancement of this drug uses in therapy. For that, in this present work, a new approach joining two different methodologies, previously applied to organic compounds, has been developed and validated for the thorough characterization of some complex organic compounds such as the natural bioactive *t*-DCTN.

Conclusions

The crystallographic and theoretical data are in agreement with the previously detailed NMR analysis and characterization of the structure of *t*-DCTN. Experimental and theoretical geometric parameters present nearly negligible discrepancies, indicating that B3LYP/6-311G++(d,p) is a satisfactory level of theory for the calculation of the optimized geometry of complex molecules such as *t*-DCTN. Those results confirmed the stereochemistry of the decaline and lactone units and a hindered rotation around the C12–C13 bond in *t*-DCTN.

There are very good correlations involving experimental and theoretical magnetic properties (NMR nuclear shielding and spin-spin coupling constants), indicating that: (1) the B3LYP/6-311G++(d,p)/GIAO method is satisfactory for the calculation of NMR nuclear shielding and; (2) the B3LYP/311G++(d,p)/GIAO method is satisfactory for the calculation of spin-spin coupling constants.

The values of QTAIM delocalization indexes involving vicinal or long range hydrogen atoms correlate well with both corresponding theoretical and experimental spin-spin

coupling constants of *t*-DCTN, indicating that the amount of charge density between each proton pair (being vicinal or not) is directly proportional to the spin-spin coupling constant.

From the topological analysis of *t*-DCTN there are five intramolecular bonded interactions in *t*-DCTN (three out of them being hydrogen-hydrogen bonds) which possibly influence in the optimal nuclear configuration and the geometric structure of *t*-DCTN.

A new approach joining two different methodologies, previously applied to organic compounds, has been developed and validated in this work for the thorough characterization of complex organic compounds.

Supplementary Information

Selected bond length and bond angles from X-ray diffraction and B3LYP method, experimental and theoretical ¹H and ¹³C NMR chemical shifts, experimental and theoretical NMR spin-spin coupled constants, Z-matrix and crystallographic data for *t*-DCTN. This material is available free of charge at <http://jbcs.sq.org.br> as PDF file.

Acknowledgments

The authors are grateful to FAPERN (Fundação de Amparo à Pesquisa do Estado do Rio Grande do Norte), CAPES (Coordenação de Aperfeiçoamento de Pessoal de Nível Superior) and CNPq (Conselho Nacional de Desenvolvimento Científico e Tecnológico) for financial support.

References

1. Murthy, M. M.; Subramanyam, M.; Bindu, M. H.; Annapurna, J.; *Fitoterapia* **2005**, *76*, 336.
2. Shirota, O.; Nagamatsu, K.; Sekita, S.; *J. Nat. Prod.* **2006**, *69*, 1782.
3. Brasil, D. S. B.; Alves, C. N.; Guilhon, G. M. S. P.; Muller, A. H.; Secco, R. S.; Peris, G.; Llusar, R.; *Int. J. Quan. Chem.* **2008**, *108*, 2564.
4. Ravikumar, Y. S.; Mahadevan, K. M.; Manjunatha, H.; Satyanarayana, N. D.; *Phytomedicine* **2010**, *17*, 513.
5. Maciel, M. A. M.; Pinto, A. C.; Arruda, A. C.; Pamplona, S. G.; Vanderlinde, F. A.; Lapa, A. J.; Echevarria, A.; Grynberg, N. F.; Cólus, I. M. S.; Farias, R. A. F.; Costa, A. M. L.; Rao, V. S. N.; *J. Ethnopharmacol.* **2000**, *70*, 41.
6. Costa, M. P.; Magalhães, N. S. S.; Gomes, F. E. S.; Maciel, M. A. M.; *Braz. J. Pharmacog.* **2007**, *17*, 275.
7. Ågner, A. R.; Maciel, M. A. M.; Pinto, A. C.; Pamplona, S. G.; Cólus, I. M.; *Teratogen. Carcin. Mut.* **1999**, *19*, 377.

8. Poersch, A.; Santos, F. V.; Maciel, M. A. M.; Câmara, J. K. P.; Dantas, T. N. C.; Cólus, I. M. S.; *Mutat. Res.* **2007**, *629*, 14.
9. Ferguson, G.; Marsh, W. C.; *Cryst. Struct. Commun.* **1976**, *5*, 35.
10. Herz, W.; Pilotti, A. M.; Soderholm, A. C.; Shuhama, I. K.; Vichnewski, W.; *J. Org. Chem.* **1977**, *42*, 3913.
11. Busygin, I.; Nieminen, V.; Taskinen, A.; Sinkkonen, J.; Toukoniitty, E.; Sillanpaa, R.; Murzin, D. Y.; Leino, R.; *J. Org. Chem.* **2008**, *73*, 6559.
12. Roslund, M. U.; Klika, K. D.; Lehtila, R. L.; Tahtinen, P.; Sillanpaa, R.; Leino, R.; *J. Org. Chem.* **2004**, *69*, 18.
13. Nishino, C.; Manabe, S.; Kazui, M.; Matsuzaki, T.; *Tetrahedron Lett.* **1984**, *25*, 2809.
14. Soriano-Garcia, M.; Toscano, R. A.; Esquivel, B.; Hernandez, M.; Rodriguez-Hahn, L.; *Acta Crystallogr., Sect. C: Cryst. Struct. Commun.* **1987**, *43*, 272.
15. Manriquez, V.; San-Martin, A.; Rovirosa, R.; von Schnering, H. G.; Peters, K. *Acta Crystallogr., Sect. C: Cryst. Struct. Commun.* **1990**, *46*, 1170.
16. Ning, X.; Zhi-Da, M.; Shou-Xun, Z.; Bing, W.; Qi-Tai, Z.; Pei, Z.; *Phytochemistry* **1991**, *30*, 1963.
17. Toscano, R. A.; Sanchez, A. A.; Esquivel, B.; Esquivel, O.; Rodriguez-Hahn, L.; *Acta Crystallogr., Sect. C: Cryst. Struct. Commun.* **1994**, *50*, 1794.
18. Huan-Ming, C.; Zhi-Da, M.; Iinuma, M.; Tanaka, T.; *Heterocycles* **1996**, *43*, 611.
19. Ye, D.; Shu-Lin, P.; Qiang, Z.; Xun, L.; Li-Sheng, D.; *Helv. Chim. Acta* **2002**, *85*, 2547.
20. Januario, A. H.; Santos, S. L.; Marcussi, S.; Mazzi, M. V.; Pietro, R. C. R. L.; Sato, D. N.; Ellena, J.; Sampaio, S. V.; Franca, S. C.; Soares, A. M.; *Chem. Biol. Interact.* **2004**, *150*, 243.
21. Sathe, M.; Kaushik, M. P.; *Bioorg. Med. Chem. Lett.* **2010**, *20*, 1312.
22. Cantrell, C. L.; Klun, J. A.; Pridgeon, J.; Becnel, J.; Green III, S.; Fronczek, F. R.; *Chem. Biodivers.* **2009**, *6*, 447.
23. Liu, H.; Chou, G.; Guo, Y.; Ji, L.; Wang, J.; Wang, Z.; *Phytochemistry* **2010**, *71*, 1174.
24. Brasil, D. S. B.; Müller, A. H.; Guilhon, G. M. S. P.; Alves, C. N.; Peris, G.; Llusard, R.; Molina, V.; *J. Braz. Chem. Soc.* **2010**, *21*, 731.
25. Brasil, D. S. B.; Moreira, R. Y. O.; Müller, A. H.; Alves, C. N.; *Int. J. Quan. Chem.* **2006**, *106*, 2706.
26. Guo, P.; Li, Y.; Xu, J.; Liu, C.; Ma, Y.; Guo, Y.; *J. Nat. Prod.* **2011**, *74*, 1575.
27. Günther, H.; *NMR Spectroscopy: Basic Principles. Concepts and Applications in Chemistry*, 2nd ed.; John Wiley & Sons: New York, 1995.
28. Muller, N.; Pritchard, D. E.; *J. Chem. Phys.* **1959**, *31*, 768.
29. Karplus, M.; Anderson, D. H.; *J. Chem. Phys.* **1959**, *30*, 6.
30. Karplus, M.; *J. Chem. Phys.* **1959**, *30*, 11.
31. Karplus, M.; *J. Am. Chem. Soc.* **1963**, *85*, 2870.
32. Barone, V.; Peralta, J. E.; Contreras, R. H.; Snyder, J. P.; *J. Phys. Chem. A.* **2002**, *106*, 5607.
33. Pihlaja, K.; Tahtinen, P.; Klika, K. D.; Jokela, T.; Salakka, A.; Wahala, K.; *J. Org. Chem.* **2003**, *68*, 6864.
34. Bally, T.; Rablen, P. R.; *J. Org. Chem.* **2011**, *76*, 4818.
35. López-Vallejo, F.; Fragoso-Serrano, M.; Suárez-Ortiz, G. A.; Hernández-Rojas, A. C.; Cerda-García-Rojas, C. M.; Pereda-Miranda, R.; *J. Org. Chem.* **2011**, *76*, 6057.
36. Pu, J.; Huang, S.; Ren, J.; Xiao, W.; Li, L. M.; Li, R.; Li, L. B.; Liao, T.; Lou, L.; Zhu, H.; Sun, H.; *J. Nat. Prod.* **2007**, *70*, 1706.
37. Sánchez-Mendoza, E.; Hernández-Trujillo, J.; del Río-Portilla, F.; *J. Phys. Chem. A.* **2007**, *111*, 8264.
38. Del Bene, J. E.; Alkorta, I.; Elguero, J.; *J. Phys. Chem. A.* **2010**, *114*, 3713.
39. Alkorta, I.; Elguero, J.; Limbach, H.; Shenderovich, I. G.; Winkler, T.; *Magn. Reson. Chem.* **2009**, *47*, 585.
40. Czernek, J.; Lang, J.; Sklenář, V.; *J. Phys. Chem. A.* **2000**, *104*, 2788.
41. Gräfenstein, J.; Tuttle, T.; Cremer, D.; *Phys. Chem. Chem. Phys.* **2005**, *7*, 452.
42. Gräfenstein, J.; Kraka, E.; Cremer, D.; *J. Phys. Chem. A.* **2004**, *108*, 4520.
43. Bouř, P.; Raich, I.; Kaminský, J.; Hrabal, R.; Čejka, J.; Sychrovský, V.; *J. Phys. Chem. A.* **2004**, *108*, 6365.
44. Ramsey, N. F.; Purcell, E. M.; *Phys. Rev.* **1952**, *85*, 143.
45. Ramsey, N. F.; *Phys. Rev.* **1953**, *91*, 303.
46. Autschbach, J.; Le Guennic, B.; *J. Chem. Ed.* **2007**, *84*, 156.
47. Cremer, D.; Gräfenstein, J.; *Phys. Chem. Chem. Phys.* **2007**, *9*, 2791.
48. Helgaker, T.; Watson, M.; Handy, N. C.; *J. Chem. Phys.* **2000**, *113*, 9402.
49. Sychrovský, V.; Gräfenstein, J.; Cremer, D.; *J. Chem. Phys.* **2000**, *113*, 3530.
50. Bader, R. F. W.; Streitwieser, A.; Neuhaus, A.; Laidig, K. E.; Speers, P.; *J. Am. Chem. Soc.* **1996**, *118*, 4959.
51. Bader, R. F. W.; *Atoms in Molecules: A Quantum Theory*; Oxford University Press: Oxford, 1994.
52. Haiduke, R. L. A.; de Oliveira, A. E.; Bruns, R. E.; *J. Phys. Chem. A.* **2004**, *108*, 6788.
53. Haiduke, R. L. A.; Bruns, R. E.; *J. Phys. Chem. A.* **2005**, *109*, 2680.
54. Bader, R. F. W.; Keith, T. A.; *J. Chem. Phys.* **1993**, *99*, 3683.
55. Koritsanszky, T. S.; Coppens, P.; *Chem. Rev.* **2001**, *101*, 1583.
56. Matta, C. F.; Hernández-Trujillo, J.; Bader, R. F. W.; *J. Phys. Chem. A.* **2002**, *106*, 7369.
57. Mandado, M.; Blockhuys, F.; Alsenoy, C. V.; *Chem. Phys. Lett.* **2006**, *430*, 454.
58. Sánchez-Mendoza, E.; Hernández-Trujillo, J.; *Magn. Reson. Chem.* **2010**, *48*, 866.
59. Castillo, N.; Matta, C. F.; Boyd, R. J.; *J. Chem. Inf. Mod.* **2005**, *45*, 354.

60. Maciel, M. A. M.; Pinto, A. C.; Kaiser, C. R.; *Magn. Reson. Chem.* **2003**, *41*, 278.
61. Enraf-Nonius; *CAD-4 Software*; Enraf-Nonius, Delft, The Netherlands, 1989.
62. Altomare, A.; Burla, M. C.; Camalli, M.; Cascarano, G.; Giacovazzo, C.; Guagliardi, A.; Moliterni, A. G. G.; Spagna, R.; *J. Appl. Crystallogr.* **1999**, *32*, 115.
63. Sheldrick, G.; *SHELXL-97 Program for Crystal Structure Refinement*; University of Göttingen, Germany, 1997.
64. Spek, A. L.; *Acta Crystallogr., Sect. D: Biol. Crystallogr.* **2009**, *65*, 148.
65. Fletcher, R.; *Practical Methods of Optimization*; Wiley: New York, 1980.
66. Becke, A. D.; *J. Chem. Phys.* **1993**, *98*, 5648.
67. Becke, A. D.; *J. Chem. Phys.* **1993**, *98*, 1372.
68. Dunning, J. T. H.; *J. Chem. Phys.* **1989**, *90*, 1007.
69. Head-Gordon, M.; Pople, J. A.; Frisch, M. J.; *Chem. Phys. Lett.* **1988**, *153*, 503.
70. Frisch, M. J.; Head-Gordon, M.; Pople, J. A.; *Chem. Phys. Lett.* **1990**, *166*, 281.
71. Frisch, M. J.; Head-Gordon, M.; Pople, J. A.; *Chem. Phys. Lett.* **1990**, *166*, 275.
72. Frisch, M. J.; Trucks, G. W.; Schlegel, H. B.; Scuseria, G. E.; Robb, M. A.; Cheeseman, J. R.; Scalmani, G.; Barone, V.; Mennucci, B.; Petersson, G. A.; Nakatsuji, H.; Caricato, M.; Li, X.; Hratchian, H. P.; Izmaylov, A. F.; Bloino, J.; Zheng, G.; Sonnenberg, J. L.; Hada, M.; Ehara, M.; Toyota, K.; Fukuda, R.; Hasegawa, J.; Ishida, M.; Nakajima, T.; Honda, Y.; Kitao, O.; Nakai, H.; Vreven, T.; Montgomery, J. A., Jr.; Peralta, J. E.; Ogliaro, F.; Bearpark, M.; Heyd, J. J.; Brothers, E.; Kudin, K. N.; Staroverov, V. N.; Kobayashi, R.; Normand, J.; Raghavachari, K.; Rendell, A.; Burant, J. C.; Iyengar, S. S.; Tomasi, J.; Cossi, M.; Rega, N.; Millam, N. J.; Klene, M.; Knox, J. E.; Cross, J. B.; Bakken, V.; Adamo, C.; Jaramillo, J.; Gomperts, R.; Stratmann, R. E.; Yazyev, O.; Austin, A. J.; Cammi, R.; Pomelli, C.; Ochterski, J. W.; Martin, R. L.; Morokuma, K.; Zakrzewski, V. G.; Voth, G. A.; Salvador, P.; Dannenberg, J. J.; Dapprich, S.; Daniels, A. D.; Farkas, Ö.; Foresman, J. B.; Ortiz, J. V.; Cioslowski, J.; Fox, D. J.; *Gaussian 09, Rev A.02*; Gaussian, Inc.: Wallingford, CT, 2009.
73. Biegler-König, F.; Schönbohm, J.; Bayles, D.; *J. Comput. Chem.* **2001**, *22*, 545.
74. Jackson, P. L.; North, H.; Alexander, M. S.; Assey, G. E.; Scott, K. R.; Butcher, R. J.; *Acta Crystallogr., Sect. E: Struct. Rep. Online*. 2011, *67*, 2272.
75. Gutowsky, H. S.; McCall, D. W.; Slichter, C. P.; *Phys. Rev.* **1952**, *84*, 589.
76. Blake, P. R.; Lee, B.; Summers, M. F.; Adams, M. W. W.; Park, J. B.; Zhou, Z. H.; Bax, A.; *J. Biomol. NMR* **1992**, *2*, 527.
77. Blake, P. R.; Park, J. B.; Adams, M. W. W.; Summers, M. F.; *J. Am. Chem. Soc.* **1992**, *114*, 4931.
78. Bader, R. F. W.; Essén, H.; *J. Chem. Phys.* **1984**, *80*, 1943.
79. Espinosa, E.; Alkorta, I.; Elguero, J.; Molins, E.; *J. Chem. Phys.* **2002**, *117*, 5529.
80. Gibbs, G. V.; Spackman, M. A.; Jayatilaka, D.; Rosso, K. M.; Cox, D. F.; Tech, V.; *J. Phys. Chem. A* **2006**, *110*, 12259.
81. Matta, C. F.; Hernández-Trujillo, J.; Tang, T.; Bader, R. F. W.; *Chem. Eur. J.* **2003**, *9*, 1940.
82. Firme, C. L.; Pontes, D. D. L.; Antunes, O. A. C.; *Chem. Phys. Lett.* **2010**, *499*, 193.
83. Hernández-Trujillo, J.; Matta, C. F.; *Struct. Chem.* **2007**, *18*, 849.
84. Mariam, Y. H.; Musin, R. N.; *J. Phys. Chem. A* **2008**, *112*, 134.
85. Lapenda, T. L. S.; Morais, W. A.; Almeida, F. J. F.; Ferraz, M. S.; Lira, M. C. B.; Santos, N. P. S.; Maciel, M. A. M.; Santos-Magalhães, N. S.; *J. Biomed. Nanotechnol.* **2013**, *9*, 499.
86. Nascimento-Filho, J. M.; de Melo, C. P.; Santos-Magalhães, V. R.; Maciel, M. A. M.; Andrade, C. A. S.; *Colloids Surf., A* **2010**, *358*, 42.
87. Canegim, B. H.; Serpeloni, J. M.; Maciel, M. A. M.; Cólus, I. M. S.; Mesquita, S. F. P.; *J. Med. Plants Res.* **2011**, *5*, 3277.
88. Lapenda, T. L. S.; Morais, W. A.; Lira, M. C. B.; Maciel, M. A. M.; Santos-Magalhães, N. S.; *Lat. Am. J. Pharm.* **2012**, *31*, 97.

Submitted: August 4, 2013

Published online: January 17, 2014

Supplementary Information

Experimental and NMR Theoretical Methodology Applied to Geometric Analysis of the Bioactive Clerodane *trans*-Dehydrocrotonin

Breno Almeida Soares,^a Caio Lima Firme,^{*,a} Maria Aparecida Medeiros Maciel,^{a,b}
 Carlos R. Kaiser,^c Eduardo Schilling^d and Adailton J. Bortoluzzi^d

^aUniversidade Federal do Rio Grande do Norte, Instituto de Química, Campus Lagoa Nova, 59072-970 Natal-RN, Brazil

^bPrograma de Pós-graduação em Biotecnologia, Universidade Potiguar Laureate International Universities, Campus Salgado Filho, 59075-000 Natal-RN, Brazil

^cUniversidade Federal do Rio de Janeiro, Instituto de Química, Ilha do Fundão, 21941-909 Rio de Janeiro-RJ, Brazil

^dUniversidade Federal de Santa Catarina, Departamento de Química, Campus Universitário Trindade, 88040-900 Florianópolis-SC, Brazil

Bond length and bond angles data for *t*-DCTN

Table S1. Selected bond length and bond angles of *t*- DCTN from X-ray diffraction and B3LYP method

Atoms	Bond length /Å		Atoms	Bond angles /°	
	X-ray	B3LYP		X-ray	B3LYP
C1–C2	1.506	1.519	C2–C1–C10	113.0	111.9
C1–C10	1.523	1.536	O1–C2–C3	122.5	122.3
C2–O1	1.215	1.220	O1–C2–C1	121.4	121.5
C2–C3	1.449	1.466	C3–C2–C1	116.0	116.1
C3–C4	1.325	1.347	C4–C3–C2	124.1	123.2
C4–C18	1.501	1.504	C3–C4–C18	120.0	120.0
C4–C5	1.506	1.522	C3–C4–C5	121.5	121.9
C5–C6	1.525	1.537	C18–C5–C4	118.5	118.0
C5–C10	1.539	1.548	C4–C5–C6	113.0	113.5
C6–C7	1.521	1.527	C4–C5–C10	111.1	111.3
C7–C8	1.508	1.533	C6–C5–C10	110.0	110.7
C8–C17	1.538	1.535	C7–C6–C5	110.4	110.7
C8–C9	1.545	1.578	C8–C7–C6	113.2	112.5
C9–C20	1.526	1.536	C7–C8–C17	109.7	110.3
C9–C11	1.544	1.547	C7–C8–C9	113.4	112.5
C9–C10	1.546	1.565	C17–C8–C9	114.1	114.0
C11–C12	1.523	1.544	C20–C9–C11	101.6	102.6
C12–C13	1.466	1.491	C20–C9–C8	111.6	110.5
C12–O3	1.470	1.459	C11–C9–C8	112.5	111.8
C13–C16	1.343	1.361	C20–C9–C10	110.3	110.8
C13–C14	1.424	1.440	C11–C9–C10	112.5	111.8
C15–O4	1.358	1.364	C8–C9–C10	110.5	110.0
C16–O4	1.347	1.358	C1–C10–C5	109.2	109.2
C20–O2	1.200	1.203	C1–C10–C9	113.0	113.5
C20–O3	1.346	1.353	C5–C10–C9	114.3	114.0
			C12–C11–C9	106.9	105.7
			C13–C12–O3	110.4	109.9
			O3–C12–C11	103.1	105.0
			C16–C13–C14	103.3	105.7
			C16–C13–C12	125.5	125.7
			C15–C14–C13	108.4	106.2
			C14–C15–O4	109.8	110.5
			C13–C16–O4	112.9	110.7
			O2–C20–O3	120.5	121.3
			O2–C20–C9	128.1	127.4
			O3–C20–C9	111.4	111.2
			C20–O3–C12	111.8	112.2
			C16–O4–C15	105.6	106.8

*e-mail: firme.caio@gmail.com, caiofirme@quimica.ufrn.br

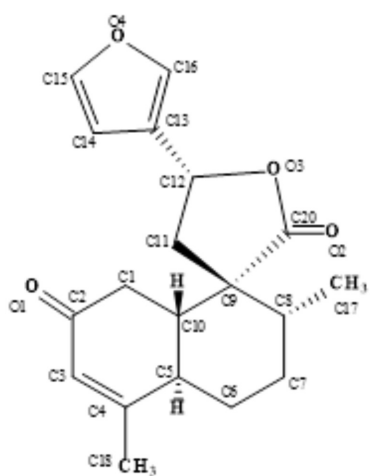
**¹H and ¹³C NMR chemical shift data, in ppm,
for *t*-DCTN**

Following the IUPAC diterpene numeration rule, both carbon (C) and hydrogen (H) atoms have the same numeration. The numbered skeleton structure of *t*-DCTN is indicated below Table S2.

Table S2. Experimental⁵⁹ and theoretical ¹H and ¹³C NMR chemical shifts (ppm) for *t*-DCTN

Atoms	Experimental		Theoretical	
	δC	δH	δC	δH
1(p)a	39.76	2.19	48.71	2.38
1(p)e		2.54		2.70
2	197.50	–	206.96	–
3	126.73	5.89	138.58	6.19
4	165.70	–	180.28	–
5	39.59	3.18	49.84	3.42
6a	28.23	1.18	38.44	1.21
6e		2.27		2.32
7a	30.13	1.88	39.43	2.20
7e		1.66		1.56
8	41.74	1.69	54.05	1.59
9	51.40	–	63.10	–
10	46.11	1.81	57.73	1.67
11	40.53	2.42	51.67	2.49
11'		2.37		2.09
12	72.31	5.43	82.50	5.33
13	125.06	–	138.87	–
14	107.98	6.41	119.78	6.91
15	144.26	7.45	156.99	7.78
16	139.93	7.46	152.59	7.69
17	17.57	1.16	24.24	1.43
18	21.90	1.97	29.96	2.07
20	176.90	–	188.61	–

a: axial; e: equatorial; (p): pseudo (related to some hydrogens of decalin).



NMR spin-spin coupling constant data for *t*-DCTN

Table S3. Experimental⁵⁹ and theoretical (B3LYP/6-311++(d,p)) NMR spin-spin coupling constants and delocalization indexes (DI) for hydrogen pairs in *t*-DCTN.

H pairs	$(J_2-J_4) / \text{Hz}$		DI $\times 10^3 / \text{a.u.}$
	Experimental	B3LYP	
H1(p)a–H10	13.8	12.13	12.096
H1(p)e–H10	2.8	2.71	2.662
H3–H18	1.27	1.96	1.245
H3–H5	1.19	2.99	1.253
H5–H6a	12.5	10.51	11.098
H5–H10	10.7	8.42	10.546
H5–H6e	3.35	3.58	3.328
H5–H18	1.2	2.07	2.303
H6a–H7a	12.7	11.41	11.808
H6a–H7e	3.61	3.51	4.134
H6e–H7a	3.6	3.601	3.882
H6e–H7e	3.3	3.13	3.765
H7a–H8	12.31	10.5	11.877
H7e–H8	3.58	3.38	3.991
H8–H17	6.8	3.61	3.531
H11- H12	8.62	7.82	6.998
H11'- H12	8.65	8.1	7.309
H14–H15	1.83	1.72	2.101
H14–H16	0.89	0.34	1.651
H15–H16	1.66	0.87	1.919

a: axial; e: equatorial; (p): pseudo (related to some hydrogens of decalin).

Z-Matrix structure for t -DCTN

0	1					
C						
C	1	B1				
C	2	B2	1	A1		
C	3	B3	2	A2	1	D1
C	4	B4	3	A3	2	D2
C	1	B5	2	A4	3	D3
H	4	B6	3	A5	2	D4
H	4	B7	3	A6	2	D5
H	6	B8	1	A7	2	D6
C	3	B9	2	A8	1	D7
C	2	B10	1	A9	6	D8
H	11	B11	2	A10	1	D9
H	11	B12	2	A11	1	D10
C	11	B13	2	A12	1	D11
H	14	B14	11	A13	2	D12
H	14	B15	11	A14	2	D13
C	14	B16	11	A15	2	D14
H	17	B17	14	A16	11	D15

C	1	B18	6	A17	5	D16	B24	1.09333367
H	19	B19	1	A18	6	D17	B25	1.09333296
H	19	B20	1	A19	6	D18	B26	1.54470272
H	19	B21	1	A20	6	D19	B27	1.09139224
C	17	B22	14	A21	11	D20	B28	1.08851816
H	23	B23	17	A22	14	D21	B29	1.53957138
H	23	B24	17	A23	14	D22	B30	1.54629218
H	23	B25	17	A24	14	D23	B31	1.35438936
C	10	B26	3	A25	2	D24	B32	1.20106107
H	27	B27	10	A26	3	D25	B33	1.09250505
H	27	B28	10	A27	3	D26	B34	1.49165820
C	10	B29	3	A28	2	D27	B35	1.36102398
C	27	B30	10	A29	3	D28	B36	2.18706738
O	30	B31	10	A30	3	D29	B37	1.07745495
O	30	B32	10	A31	3	D30	B38	1.07667935
H	31	B33	27	A32	10	D31	B39	1.21874690
C	31	B34	27	A33	10	D32	B40	1.35577876
C	35	B35	31	A34	27	D33	B41	1.07837670
C	36	B36	35	A35	31	D34	B42	1.35920779
H	36	B37	35	A36	31	D35	B43	1.07000000
H	37	B38	36	A37	35	D36	B44	1.07000000
O	5	B39	4	A38	3	D37	A1	113.69588071
C	37	B40	36	A39	35	D38	A2	112.64210726
H	41	B41	37	A40	36	D39	A3	111.84531507
O	36	B42	35	A41	31	D40	A4	122.44597069
H	3	B43	2	A42	1	D41	A5	111.31552864
H	2	B44	1	A43	6	D42	A6	112.05433055
						A7		120.97398975
B1	1.51803783					A8		111.53177287
B2	1.54061592					A9		111.14452881
B3	1.53193224					A10		109.51941125
B4	1.52007448					A11		109.16619218
B5	1.34608977					A12		112.18388730
B6	1.09728912					A13		109.46432109
B7	1.09256316					A14		110.76530116
B8	1.08574024					A15		111.71633951
B9	1.56993713					A16		107.30883347
B10	1.55661404					A17		120.73610018
B11	1.09383555					A18		111.75825039
B12	1.09449277					A19		110.39045683
B13	1.54115916					A20		111.30366213
B14	1.09400100					A21		111.27684777
B15	1.09367837					A22		112.64710119
B16	1.53322782					A23		109.58903837
B17	1.09778594					A24		111.67937182
B18	1.50502647					A25		116.44383240
B19	1.09394349					A26		112.83141147
B20	1.09618721					A27		111.87197251
B21	1.09068923					A28		107.53053162
B22	1.53524731					A29		105.43180834
B23	1.09273484					A30		111.17150742

A31	126.99016135	D39	-178.54842871
A32	110.89217926	D40	-178.68946042
A33	115.66090559	D41	101.87341666
A34	125.89934788	D42	-69.70769645
A35	74.06765611		
A36	133.09204790		
A37	152.39385804		
A38	121.97161267		
A39	74.03234761		
A40	126.16683329		
A41	110.73877362	_audit_creation_method	SHELXL-97
A42	75.96629185	_chemical_name_systematic	
A43	72.35721771	;	
D1	37.54160444	?	
D2	-52.92819769	;	
D3	-8.25901089	_chemical_name_common	?
D4	64.67609839	_chemical_melting_point	?
D5	-174.70620113	_chemical_formula_moiety	'C19 H22 O4'
D6	176.89299873	_chemical_formula_sum	
D7	167.91964740	'C19 H22 O4'	
D8	-131.29385604	_chemical_formula_weight	314.37
D9	-80.26247743		
D10	36.20283290		
D11	157.31493184	loop_	
D12	153.26980256	_atom_type_symbol	
D13	-89.85979495	_atom_type_description	
D14	31.91852487	_atom_type_scat_dispersion_real	
D15	49.47923124	_atom_type_scat_dispersion_imag	
D16	173.36010050	_atom_type_scat_source	
D17	116.48343566	'C' 'C' 0.0033 0.0000	
D18	-125.04497806	'International Tables Vol C Tables 4.2.6.8 and 6.1.1.4'	
D19	-4.71117747	'H' 'H' 0.0000 0.0000	
D20	166.33689976	'International Tables Vol C Tables 4.2.6.8 and 6.1.1.4'	
D21	-176.04242096	'O' 'O' 0.0106 0.0000	
D22	-57.03521595	'International Tables Vol C Tables 4.2.6.8 and 6.1.1.4'	
D23	62.01254246		
D24	-92.06387423	_symmetry_cell_setting	orthorhombic
D25	103.77711042	_symmetry_space_group_name_H-M	'P 21 21 21'
D26	-17.24782738	_symmetry_space_group_name_Hall	'P 2ac 2ab'
D27	154.05896017		
D28	-135.44106634	loop_	
D29	134.43272039	_symmetry_equiv_pos_as_xyz	
D30	-45.88150421	'x, y, z'	
D31	-94.57220085	'-x+1/2, -y, z+1/2'	
D32	141.18187816	'x+1/2, -y+1/2, -z'	
D33	120.13365900	'-x, y+1/2, -z+1/2'	
D34	-179.00647259		
D35	1.28643125	_cell_length_a	7.3869(8)
D36	-178.85908031	_cell_length_b	13.8966(13)
D37	-145.26477332	_cell_length_c	16.018(3)
D38	-0.07136514	_cell_angle_alpha	90.00
		_cell_angle_beta	90.00

`_cell_angle_gamma` 90.00
`_cell_volume` 1644.3(4)
`_cell_formula_units_Z` 4
`_cell_measurement_temperature` 293(2)
`_cell_measurement_reflns_used` 25
`_cell_measurement_theta_min` 4.92
`_cell_measurement_theta_max` 12.03

`_exptl_crystal_description` 'irregular'
`_exptl_crystal_colour` colorless
`_exptl_crystal_size_max` 0.40
`_exptl_crystal_size_mid` 0.33
`_exptl_crystal_size_min` 0.30
`_exptl_crystal_density_meas` ?
`_exptl_crystal_density_diffrn` 1.270
`_exptl_crystal_density_method` 'not measured'
`_exptl_crystal_F_000` 672
`_exptl_absorpt_coefficient_mu` 0.088
`_exptl_absorpt_correction_type` none
`_exptl_absorpt_correction_T_min` ?
`_exptl_absorpt_correction_T_max` ?
`_exptl_absorpt_process_details` ?

`_exptl_special_details`
; ? ;

`_diffrn_ambient_temperature` 293(2)
`_diffrn_radiation_wavelength` 0.71073
`_diffrn_radiation_type` MoK\(\alpha\)
`_diffrn_radiation_source` 'fine-focus sealed tube'
`_diffrn_radiation_monochromator` graphite
`_diffrn_measurement_device_type` ?
`_diffrn_measurement_method` \(\lambda w - 2\lambda q\)
`_diffrn_detector_area_resol_mean` ?
`_diffrn_standards_number` 3
`_diffrn_standards_interval_count` 200
`_diffrn_standards_interval_time` ?
`_diffrn_standards_decay_%` 1
`_diffrn_reflns_number` 2184
`_diffrn_reflns_av_R_equivalents` 0.0000
`_diffrn_reflns_av_sigmaI/netI` 0.0756
`_diffrn_reflns_limit_h_min` -9
`_diffrn_reflns_limit_h_max` 0
`_diffrn_reflns_limit_k_min` -18
`_diffrn_reflns_limit_k_max` 0
`_diffrn_reflns_limit_l_min` -21
`_diffrn_reflns_limit_l_max` 0
`_diffrn_reflns_theta_min` 1.94
`_diffrn_reflns_theta_max` 27.97

`_reflns_number_total` 2184
`_reflns_number_gt` 940
`_reflns_threshold_expression` >2\(\sigma(I)\)

`_computing_data_collection` ?
`_computing_cell_refinement` ?
`_computing_data_reduction` ?
`_computing_structure_solution` ?
`_computing_structure_refinement` 'SHELXL-97
(Sheldrick, 2008)'
`_computing_molecular_graphics` ?
`_computing_publication_material` ?

`_refine_ls_structure_factor_coef` Fsqd
`_refine_ls_matrix_type` full
`_refine_ls_weighting_scheme` calc
`_refine_ls_weighting_details`
'calc w=1/[s^2^(Fo^2)+(0.0573P)^2+0.0000P] where
P=(Fo^2+2Fc^2)/3'
`_atom_sites_solution_primary` direct
`_atom_sites_solution_secondary` difmap
`_atom_sites_solution_hydrogens` geom
`_refine_ls_hydrogen_treatment` constr
`_refine_ls_extinction_method` none
`_refine_ls_extinction_coef` ?
`_chemical_absolute_configuration` unk
`_refine_ls_number_reflns` 2184
`_refine_ls_number_parameters` 208
`_refine_ls_number_restraints` 0
`_refine_ls_R_factor_all` 0.1753
`_refine_ls_R_factor_gt` 0.0502
`_refine_ls_wR_factor_ref` 0.1386
`_refine_ls_wR_factor_gt` 0.1076
`_refine_ls_goodness_of_fit_ref` 0.986
`_refine_ls_restrained_S_all` 0.986
`_refine_ls_shift/su_max` 0.000
`_refine_ls_shift/su_mean` 0.000

loop_
`_atom_site_label`
`_atom_site_type_symbol`
`_atom_site_fract_x`
`_atom_site_fract_y`
`_atom_site_fract_z`
`_atom_site_U_iso_or_equiv`
`_atom_site_adp_type`
`_atom_site_occupancy`
`_atom_site_symmetry_multiplicity`
`_atom_site_calc_flag`
`_atom_site_refinement_flags`
`_atom_site_disorder_assembly`

_atom_site_disorder_group
C1 C 0.2078(6) 0.6281(3) 0.0303(2) 0.0632(11)
Uani 1 1 d ...
H1A H 0.2704 0.5694 0.0147 0.076 Uiso 1 1 calc R ..
H1B H 0.0808 0.6125 0.0379 0.076 Uiso 1 1 calc R ..
C2 C 0.2253(6) 0.7000(3) -0.0396(3) 0.0655(12)
Uani 1 1 d ...
C3 C 0.2256(6) 0.8004(3) -0.0152(3) 0.0714(13)
Uani 1 1 d ...
H3 H 0.2399 0.8465 -0.0569 0.086 Uiso 1 1 calc R ..
C4 C 0.2067(6) 0.8308(3) 0.0627(3) 0.0693(12)
Uani 1 1 d ...
C5 C 0.1948(6) 0.7613(3) 0.1346(2) 0.0631(11)
Uani 1 1 d ...
H5 H 0.0662 0.7487 0.1450 0.076 Uiso 1 1 calc R ..
C6 C 0.2756(7) 0.8012(3) 0.2151(3) 0.0840(14)
Uani 1 1 d ...
H6A H 0.4029 0.8154 0.2067 0.101 Uiso 1 1 calc R ..
H6B H 0.2147 0.8607 0.2299 0.101 Uiso 1 1 calc R ..
C7 C 0.2551(7) 0.7288(4) 0.2857(3) 0.0896(15)
Uani 1 1 d ...
H7A H 0.3100 0.7551 0.3358 0.108 Uiso 1 1 calc R ..
H7B H 0.1272 0.7194 0.2970 0.108 Uiso 1 1 calc R ..
C8 C 0.3404(6) 0.6327(4) 0.2667(3) 0.0796(14)
Uani 1 1 d ...
H8 H 0.4706 0.6445 0.2606 0.095 Uiso 1 1 calc R ..
C9 C 0.2761(5) 0.5887(3) 0.1832(2) 0.0618(11)
Uani 1 1 d ...
C10 C 0.2845(6) 0.6646(3) 0.1127(2) 0.0562(10)
Uani 1 1 d ...
H10 H 0.4130 0.6781 0.1030 0.067 Uiso 1 1 calc R ..
C11 C 0.3874(6) 0.4977(3) 0.1627(3) 0.0728(12)
Uani 1 1 d ...
H11A H 0.4178 0.4962 0.1038 0.087 Uiso 1 1 calc R ..
H11B H 0.4987 0.4969 0.1947 0.087 Uiso 1 1 calc R ..
C12 C 0.2700(6) 0.4115(3) 0.1853(3) 0.0732(12)
Uani 1 1 d ...
H12 H 0.2979 0.3917 0.2426 0.088 Uiso 1 1 calc R ..
C13 C 0.2841(7) 0.3274(4) 0.1304(3) 0.0764(13)
Uani 1 1 d ...
C14 C 0.3384(8) 0.3191(4) 0.0454(3) 0.1034(18)
Uani 1 1 d ...
H14 H 0.3731 0.3697 0.0109 0.124 Uiso 1 1 calc R ..
C15 C 0.3313(9) 0.2267(5) 0.0238(4) 0.121(2)
Uani 1 1 d ...
H15 H 0.3619 0.2024 -0.0284 0.145 Uiso 1 1 calc R ..
C16 C 0.2486(7) 0.2361(4) 0.1525(4) 0.0949(16) Uani 1
1 d ...
H16 H 0.2114 0.2181 0.2057 0.114 Uiso 1 1 calc R ..
C17 C 0.3189(8) 0.5654(4) 0.3422(3) 0.115(2)
Uani 1 1 d ...
H17A H 0.3733 0.5043 0.3299 0.172 Uiso 1 1 calc R ..
H17B H 0.1926 0.5565 0.3540 0.172 Uiso 1 1 calc R ..
H17C H 0.3773 0.5933 0.3900 0.172 Uiso 1 1 calc R ..
C18 C 0.1881(8) 0.9364(3) 0.0805(3) 0.1055(18)
Uani 1 1 d ...
H18A H 0.1756 0.9461 0.1395 0.158 Uiso 0.50 1 calc PR ..
H18B H 0.0829 0.9609 0.0524 0.158 Uiso 0.50 1 calc PR ..
H18C H 0.2937 0.9696 0.0608 0.158 Uiso 0.50 1 calc PR ..
H18D H 0.1925 0.9717 0.0290 0.158 Uiso 0.50 1 calc PR ..
H18E H 0.2853 0.9568 0.1161 0.158 Uiso 0.50 1 calc PR ..
H18F H 0.0744 0.9482 0.1077 0.158 Uiso 0.50 1 calc PR ..
C20 C 0.0852(6) 0.5476(4) 0.1903(3) 0.0646(11)
Uani 1 1 d ...
O1 O 0.2325(5) 0.6745(2) -0.11208(19) 0.0905(10)
Uani 1 1 d ...
O2 O -0.0543(4) 0.5905(2) 0.19977(19) 0.0798(9)
Uani 1 1 d ...
O3 O 0.0855(4) 0.4511(2) 0.1829(2) 0.0809(10)
Uani 1 1 d ...
O4 O 0.2726(6) 0.1733(3) 0.0894(3) 0.1154(13)
Uani 1 1 d ...

loop_
_atom_site_aniso_label
_atom_site_aniso_U_11
_atom_site_aniso_U_22
_atom_site_aniso_U_33
_atom_site_aniso_U_23
_atom_site_aniso_U_13
_atom_site_aniso_U_12
C1 0.059(3) 0.061(2) 0.070(2) -0.003(2) 0.001(2) 0.005(2)
C2 0.055(3) 0.077(3) 0.065(3) 0.000(2) -0.001(3) -0.002(2)
C3 0.059(3) 0.066(3) 0.089(3) 0.020(3) -0.009(3) -0.010(2)
C4 0.049(3) 0.059(3) 0.100(3) -0.006(3) -0.004(3)
-0.009(2)
C5 0.047(2) 0.062(3) 0.080(3) -0.012(2) 0.005(2) -0.004(2)
C6 0.073(3) 0.086(3) 0.093(3) -0.027(3) -0.006(3)
-0.006(3)
C7 0.079(3) 0.121(4) 0.069(3) -0.023(3) 0.000(3) -0.018(4)
C8 0.065(3) 0.108(4) 0.066(3) -0.001(3) -0.005(2)
-0.010(3)
C9 0.045(2) 0.079(3) 0.061(2) 0.003(2) -0.001(2) 0.000(2)
C10 0.045(2) 0.064(2) 0.060(2) -0.003(2) 0.006(2)
-0.006(2)
C11 0.053(2) 0.085(3) 0.080(3) 0.012(3) -0.007(2) 0.002(3)
C12 0.060(3) 0.078(3) 0.082(3) 0.022(3) -0.011(3) 0.007(3)
C13 0.068(3) 0.069(3) 0.092(4) 0.019(3) -0.012(3)
-0.002(3)
C14 0.136(5) 0.086(4) 0.088(4) 0.009(3) -0.010(4) 0.002(4)
C15 0.147(6) 0.102(5) 0.113(5) 0.001(5) -0.026(4) 0.016(5)
C16 0.069(3) 0.093(4) 0.123(5) 0.029(4) -0.007(3) 0.009(3)

C17 0.119(5) 0.158(5) 0.067(3) 0.013(4) -0.014(3)
 -0.038(5)

C18 0.112(4) 0.059(3) 0.145(5) -0.013(3) -0.017(4)
 0.003(3)

C20 0.054(3) 0.077(3) 0.063(3) 0.006(3) 0.005(3) -0.006(3)

O1 0.109(3) 0.099(2) 0.0640(18) -0.0010(18) -0.006(2)
 -0.004(2)

O2 0.057(2) 0.090(2) 0.093(2) -0.0023(19) 0.0137(17)
 0.0001(18)

O3 0.063(2) 0.077(2) 0.103(3) 0.018(2) 0.009(2)
 -0.0064(19)

O4 0.102(3) 0.079(2) 0.165(4) 0.009(3) -0.025(3) 0.005(3)

loop_
 _geom_bond_atom_site_label_1
 _geom_bond_atom_site_label_2
 _geom_bond_distance
 _geom_bond_site_symmetry_2
 _geom_bond_publ_flag
 C1 C2 1.506(5) . ?
 C1 C10 1.524(5) . ?
 C2 O1 1.215(5) . ?
 C2 C3 1.450(5) . ?
 C3 C4 1.324(6) . ?
 C4 C18 1.501(6) . ?
 C4 C5 1.506(6) . ?
 C5 C6 1.526(5) . ?
 C5 C10 1.538(5) . ?
 C6 C7 1.521(6) . ?
 C7 C8 1.508(6) . ?
 C8 C17 1.538(6) . ?
 C8 C9 1.545(5) . ?
 C9 C19 1.526(6) . ?
 C9 C11 1.544(5) . ?
 C9 C10 1.547(5) . ?
 C11 C12 1.522(6) . ?
 C12 C13 1.467(6) . ?
 C12 O3 1.470(5) . ?
 C13 C16 1.343(6) . ?
 C13 C14 1.423(7) . ?
 C14 C15 1.331(7) . ?
 C15 O4 1.357(7) . ?
 C16 O4 1.346(6) . ?
 C20 O2 1.200(5) . ?
 C20 O3 1.346(5) . ?

loop_
 _geom_angle_atom_site_label_1
 _geom_angle_atom_site_label_2
 _geom_angle_atom_site_label_3
 _geom_angle

_geom_angle_site_symmetry_1
 _geom_angle_site_symmetry_3
 _geom_angle_publ_flag
 C2 C1 C10 113.0(3) . . ?
 O1 C2 C3 122.6(4) . . ?
 O1 C2 C1 121.4(4) . . ?
 C3 C2 C1 116.0(4) . . ?
 C4 C3 C2 124.1(4) . . ?
 C3 C4 C18 120.0(4) . . ?
 C3 C4 C5 121.5(4) . . ?
 C18 C4 C5 118.5(4) . . ?
 C4 C5 C6 113.0(4) . . ?
 C4 C5 C10 111.1(3) . . ?
 C6 C5 C10 110.0(3) . . ?
 C7 C6 C5 110.4(3) . . ?
 C8 C7 C6 113.2(4) . . ?
 C7 C8 C17 109.7(4) . . ?
 C7 C8 C9 113.4(4) . . ?
 C17 C8 C9 114.1(4) . . ?
 C20 C9 C11 101.6(3) . . ?
 C20 C9 C8 111.6(3) . . ?
 C11 C9 C8 110.2(4) . . ?
 C20 C9 C10 110.3(3) . . ?
 C11 C9 C10 112.4(3) . . ?
 C8 C9 C10 110.5(3) . . ?
 C1 C10 C5 109.1(3) . . ?
 C1 C10 C9 113.0(3) . . ?
 C5 C10 C9 114.3(3) . . ?
 C12 C11 C9 106.9(3) . . ?
 C13 C12 O3 110.4(4) . . ?
 C13 C12 C11 116.3(4) . . ?
 O3 C12 C11 103.1(3) . . ?
 C16 C13 C14 103.3(5) . . ?
 C16 C13 C12 125.5(5) . . ?
 C14 C13 C12 131.1(5) . . ?
 C15 C14 C13 108.4(5) . . ?
 C14 C15 O4 109.8(6) . . ?
 C13 C16 O4 112.8(5) . . ?
 O2 C20 O3 120.5(4) . . ?
 O2 C20 C9 128.0(4) . . ?
 O3 C20 C9 111.4(4) . . ?
 C20 O3 C12 111.8(4) . . ?
 C16 O4 C15 105.6(5) . . ?

_diffrn_measured_fraction_theta_max 0.962
 _diffrn_reflns_theta_full 27.97
 _diffrn_measured_fraction_theta_full 0.962
 _refine_diff_density_max 0.170
 _refine_diff_density_min -0.105
 _refine_diff_density_rms 0.031